# Inactivation of the glycine transporter 1 gene discloses vital role of glial glycine uptake in glycinergic inhibition

**Jesús Gomeza, Swen Hülsmann, Koji Ohno, Volker Eulenburg, Katalin Szöke, Diethelm Richter, Heinrich Betz**

**Angaben zur Veröffentlichung / Publication details:**

Gomeza, Jesús, Swen Hülsmann, Koji Ohno, Volker Eulenburg, Katalin Szöke, Diethelm Richter, and Heinrich Betz. 2003. "Inactivation of the glycine transporter 1 gene discloses vital role of glial glycine uptake in glycinergic inhibition." *Neuron* 40 (4): 785–96. https://doi.org/10.1016/s0896-6273(03)00672-x.

Neuron, Vol. 40, 785–796, November 13, 2003, Copyright ©2003 by Cell Press

# Inactivation of the Glycine Transporter 1 Gene Discloses Vital Role of Glial Glycine Uptake in Glycinergic Inhibition

**Jesús Gomeza,[1,3,4] Swen Hülsmann,[2,3] Koji Ohno,[1,5] Volker Eulenburg,[1] Katalin Szöke,[2] Diethelm Richter,[2] and Heinrich Betz[1,*]**

[1]Department of Neurochemistry
Max-Planck-Institute for Brain Research
Deutschordenstrasse 46
60528 Frankfurt
Germany

[2]Department of Neuro- and Sensory Physiology
University of Göttingen
Humboldtallee 23
37073 Göttingen
Germany



## Summary

**The glycine transporter subtype 1 (GlyT1) is widely expressed in astroglial cells throughout the mammalian central nervous system and has been implicated in the regulation of N-methyl-D-aspartate (NMDA) receptor activity. Newborn mice deficient in GlyT1 are anatomically normal but show severe motor and respiratory deficits and die during the first postnatal day. In brainstem slices from GlyT1-deficient mice, in vitro respiratory activity is strikingly reduced but normalized by the glycine receptor (GlyR) antagonist strychnine. Conversely, glycine or the GlyT1 inhibitor sarcosine suppress respiratory activity in slices from wild-type mice. Thus, during early postnatal life, GlyT1 is essential for regulating glycine concentrations at inhibitory GlyRs, and GlyT1 deletion generates symptoms found in human glycine encephalopathy.**

## Introduction

The amino acid glycine has important roles in both excitatory and inhibitory neurotransmission. Besides serving as an essential coagonist of glutamate at excitatory N-methyl-D-aspartate (NMDA) receptors (Johnson and Ascher, 1987; Verdoorn et al., 1987), glycine is the principal inhibitory neurotransmitter of many interneurons in spinal cord, brain stem, and some other brain regions, which are all involved in the processing of motor and sensory information (Zafra et al., 1997; Legendre, 2001). Glycine-mediated inhibition involves the uptake of the amino acid into synaptic vesicles, its exocytotic release upon depolarization-induced $Ca^{2+}$ influx, and the subsequent activation of postsynaptic strychnine-sensitive glycine receptors (GlyRs) (Betz et al., 2000). Glycinergic neurotransmission is terminated by the rapid re-uptake of glycine from the synaptic cleft. This process is mediated by $Na^+/Cl^-$-dependent glycine transporters (GlyTs) localized in the plasma membranes of neurons and surrounding glial cells (Johnston and Iversen, 1971; Lopez-Corcuera et al., 2001).

Two GlyT subtypes encoded by distinct genes, GlyT1 and GlyT2, have been identified in the mammalian central nervous system (Guastella et al., 1992; Liu et al., 1992, 1993; Smith et al., 1992). Both GlyT proteins exist in different splice variants and belong to the $Na^+/Cl^-$-dependent transporter family, a group of glycoproteins that also includes the transporters for proline, monoamines (serotonin, norepinephrine, and dopamine), and GABA (Amara and Kuhar, 1993; Schloss et al., 1994; Nelson, 1998). All of these membrane proteins share a common transmembrane topology with 12 membrane-spanning domains and cytoplasmic N- and C-terminal regions.

In situ hybridization and immunohistochemical studies have shown that GlyT1 is widely expressed in glial cells of the hippocampus, cortex, and cerebellum, as well as glial cells of the brain stem and spinal cord (Adams et al., 1995; Zafra et al., 1995a, 1995b). In contrast, GlyT2 is found predominantly in brain stem and spinal cord neurons, i.e., regions rich in glycinergic synapses (Jursky and Nelson, 1995; Zafra et al., 1995a, 1995b), and has been shown to be concentrated in the plasma membrane of axonal boutons directly apposed to GlyRs (Jursky and Nelson, 1995; Spike et al., 1997). Based on these localizations, GlyT2 is thought to provide the principal glycine uptake mechanism at inhibitory glycinergic synapses (Liu et al., 1993; Jursky and Nelson, 1995; Zafra et al., 1995a), whereas GlyT1 has been proposed to mainly function at excitatory synapses by regulating glycine levels at the coagonist binding site of NMDA receptors (Smith et al., 1992; Berger et al., 1998; Roux and Supplisson, 2000). However, due to the overlapping expression patterns of GlyT1 and GlyT2 in caudal regions of the CNS (Jursky and Nelson, 1995; Zafra et al., 1995a, 1995b) and the limited availability of GlyT antagonists that display high subtype selectivity (Lopez-Corcuera et al., 2001), the precise in vivo roles of these transporters remain to be determined.

To address this issue, we have generated knockout mice deficient in GlyT proteins. Here, we describe a mouse line that lacks functional GlyT1; mice deficient in GlyT2 are described in the accompanying paper (Gomeza et al., 2003 [this issue of *Neuron*]). GlyT1-deficient mice show severe motor and respiration deficits at birth and, unexpectedly, die during the first postnatal day, revealing a previously unrecognized vital role for GlyT1 in neonatal life. The phenotype of these newborn mice is consistent with GlyT1 being the major transporter isoform that regulates glycine concentrations at GlyRs at early stages of postnatal development. Furthermore, it mimics several of the symptoms seen in human glycine encephalopathy (also named nonketotic hyperglycinemia) and thus defines a novel animal model for this disease.

*Correspondence: neurochemie@mpih-frankfurt.mpg.de
[3]These authors contributed equally to this study.
[4]Present address: Department of Pharmacology 18.6, The Panum Institute, University of Copenhagen, DK-2200 Copenhagen, Denmark.
[5]Present address: Department of Anatomy and Neuroscience, Hamamatsu University School of Medicine, Hamamatsu, Shizuoka 431-3192, Japan.

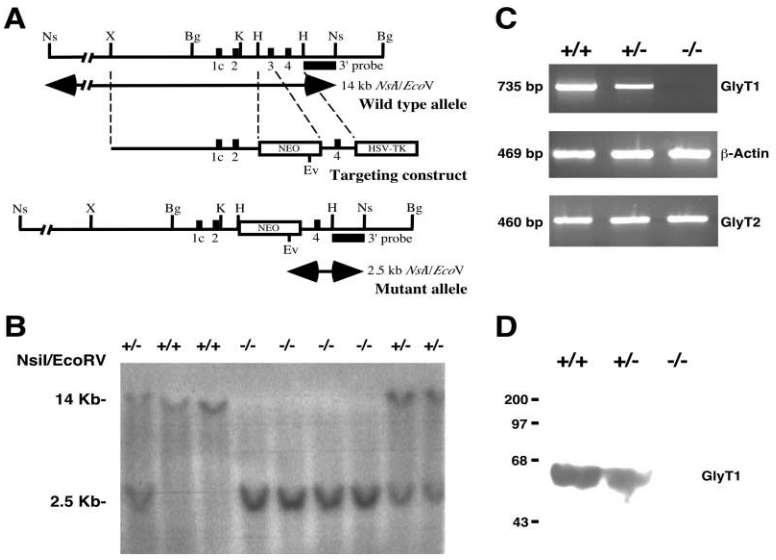


Figure 1. Targeted Disruption of the Mouse GlyT1 Gene

(A) Knockout strategy showing restriction maps of the wild-type GlyT1 locus, the targeting construct, and the targeted allele. Exons are represented as black boxes. The probe used for Southern analysis and the sizes of the restriction fragments detected with this probe are indicated. Only relevant restriction sites are shown. K, *Kpn*I; X, *Xba*I; Bg, *Bgl*II; H, *Hind*III; Ns, *Nsi*I; Ev, *Eco*RV.

(B) Genotyping of newborn F2 offspring by Southern blot analysis of *NsiI/EcoRV*-digested mouse tail DNA. The 14 kb and 2.5 kb bands represent the wild-type (+) and mutant GlyT1 (−) alleles, respectively.

(C) RT-PCR analysis of brain stem/spinal cord expression of GlyT1, β-actin, and GlyT2 in wild-type (+/+), heterozygous (+/−), and homozygous (−/−) knockout mice. Note the absence of GlyT1 transcripts in homozygous animals.

(D) Western blot analysis of brain stem/spinal cord fractions (40 μg protein/lane) using the GlyT1 antibody. GlyT1 expression was reduced in heterozygotes (+/−) and completely abolished in homozygous (−/−) knockout animals.

## Results

### Generation of GlyT1$^{-/-}$ Mice

To generate mice lacking functional GlyT1, we inactivated the GlyT1 gene (Adams et al., 1995) in mouse E14 (129/OLA) embryonic stem (ES) cells via homologous recombination. As shown in Figure 1A, a fragment of 0.37 kb encompassing exon 3, which encodes the second transmembrane region of GlyT1, was replaced by a neomycin-resistance cassette. Targeted ES cell clones were identified by Southern blot analysis, exploiting a newly introduced EcoRV site. Using an external 3′ probe, a 2.5 kb fragment was detected for the mutant allele. Two independent properly targeted ES cell clones were injected into blastocysts to generate chimeric male mice. These animals then were crossed with C57/BL6 female mice to establish germline transmission of the mutation. Mice heterozygous for the GlyT1 mutant allele (GlyT1$^{+/-}$) appeared phenotypically normal and showed undisturbed development and fertility. Intercrossing of the heterozygous mice generated wild-type (+/+), heterozygous (+/−), and homozygous (−/−) GlyT1 mutant mice. Mouse genotyping was carried out by Southern blot analysis of mouse tail DNA (Figure 1B). The homozygous mutants (GlyT1$^{-/-}$) were delivered at normal Mendelian ratios, indicating that there was no increased embryonic mortality in the mutant animals. The absence of the wild-type GlyT1 transcript and protein in the GlyT1$^{-/-}$ mice was confirmed by RT-PCR (Figure 1C) and Western blot analysis (Figure 1D), respectively.

### Glycine Transport Activity Is Reduced in GlyT1$^{-/-}$ Mice

To examine the effects of GlyT1 gene deletion more directly, high-affinity glycine uptake was measured by incubating P2 membrane fractions prepared from both forebrain and combined brainstem/spinal cord tissue of newborn mice with a final concentration of 2 μM [$^3$H]glycine. As shown in Figure 2, [$^3$H]glycine uptake was strikingly reduced, by ≥70% and ≥80% ($p < 0.001$) in the forebrain and CNS caudal regions, respectively, of GlyT1$^{-/-}$ mice, as compared to wild-type animals. This is consistent with GlyT1 being the major GlyT isoform expressed at birth (Zafra et al., 1995b; Friauf et al., 1999). P2 membrane fractions from heterozygous animals showed intermediate [$^3$H]glycine uptake values, consistent with a clear gene dosage effect of GlyT1 expression. Notably, incubation of membrane fractions from wild-

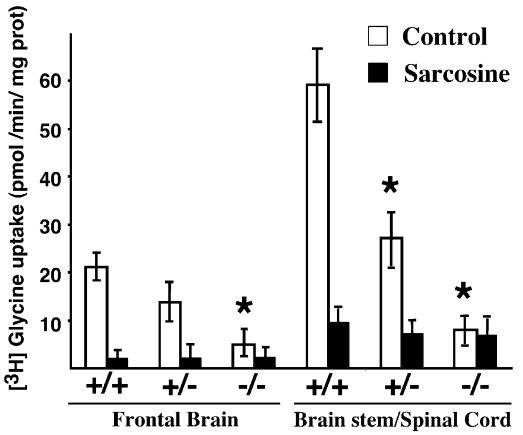


Figure 2. [$^3$H]Glycine Uptake in Different CNS Regions of Newborn Mice

Membranes were prepared from the indicated tissues of wild-type and mutant neonates and preincubated for 2 min at 37°C. Transport in the absence (control) or presence of 2 mM sarcosine was initiated by the addition of 2 μM [$^3$H]glycine in Krebs-Henseleit buffer for 1 min. Data are given as means ± SD (n = 3–4 for each genotype). Asterisk indicates significantly different from wild-type mice, $p < 0.001$ (Student's t test).

Table 1. Body Weight and Responsivity of Newborn Littermates

| Genotype (n) | GlyT1$^{+/+}$ (9) | GlyT1$^{+/-}$ (16) | GlyT1$^{-/-}$ (10) |
|---|---|---|---|
| Body weight (g) | 1.39 ± 0.09 | 1.41 ± 0.13 | 1.19 ± 0.10[a] |
| Tail pinching response | | | |
| Strong | 9 | 15 | 0 |
| Weak | 0 | 1 | 8 |
| None | 0 | 0 | 2 |

Data are expressed as means ± SD.
[a] Significantly different from the wild-type value, $p < 0.001$ (Student's t test).

type animals with 2 mM sarcosine, a specific inhibitor of GlyT1 (Lopez-Corcuera et al., 2001), decreased the uptake of [$^3$H]glycine in fractions from wild-type and heterozygous animals to values comparable to the transport activity measured in the GlyT1$^{-/-}$ membranes. These results indicate that GlyT1-mediated [$^3$H]glycine uptake is totally abolished in the homozygous mutants.

### Homozygous GlyT1$^{-/-}$ Mice Die within the First Day of Birth

Homozygous GlyT1$^{-/-}$ pups appeared externally normal but, unexpectedly, died on the day of birth, indicating that GlyT1 is dispensable for embryonic development but essential for postnatal survival. GlyT1$^{-/-}$ mice weighed ~15% less than their control littermates (Table 1), most likely because of their inability to suckle and a lack of milk in their stomachs (Figure 3A). The newborn mutant pups survived for some hours but gradually became weaker and failed to thrive, with death occurring 6–14 hr after birth. Heterozygous GlyT$^{+/-}$ animals, in contrast, developed normally, without any significant differences to wild-type littermates.

GlyT1$^{-/-}$ neonates showed only weak spontaneous motor activity. In an attempt to evaluate the neuromotor performance of the newborn pups, simple handling assays were performed. First, the response to mild tactile stimuli was tested. After being touched gently, wild-type and heterozygous neonates flailed their limbs, trying to change their body position. In contrast, GlyT1$^{-/-}$ littermates did not move upon tactile stimulation, assuming an abnormal body posture while dropping their forelimbs (Figure 3A). As a second parameter to monitor neurological reflexes, we also tested their "pinching response" behavior. When picked up and nipped by their tail, newborn mice tended to spread out their legs while producing a characteristic vocalization. As opposed to the wild-type and heterozygous neonates, the GlyT1 mutant animals only reacted weakly to strong mechanical stimuli (Table 1). In summary, GlyT1$^{-/-}$ newborn mice showed severe motosensory deficits characterized by lethargy, hypotonia, and hyporesponsivity.

Notably, GlyT1$^{-/-}$ mice exhibited severe disturbances of breathing. To measure in vivo respiratory motor activity in control and mutant mice, plethysmographic recordings were performed using a modified barometric method previously employed in neonates (Fortin et al., 1994; Chatonnet et al., 2002). Wild-type (Figure 3B) and heterozygous (not shown) newborn pups showed regu-

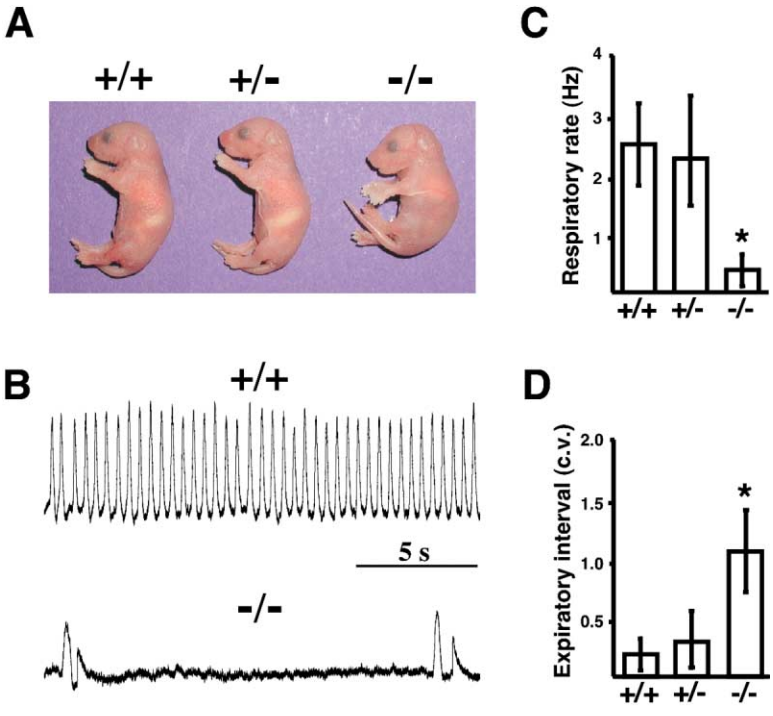


Figure 3. Phenotypical Analysis of GlyT1$^{-/-}$ Mice

(A) Compared to wild-type (+/+) and heterozygous (+/−) littermates, homozygous mutant animals (−/−) did not move spontaneously. Note that GlyT1$^{-/-}$ mice have no milk in their belly and assume an abnormal body posture with dropping forelimbs.

(B) Depression of in vivo respiratory activity in newborn GlyT1$^{-/-}$ mice. Whole-body plethysmographic recordings were obtained from wild-type (+/+) and homozygous mutant (−/−) littermates; the mutant traces shown are from a severely suppressed animal.

(C) Mean respiratory frequencies (Hz) of all genotypes analyzed.

(D) Regularity of breathing expressed by the coefficient of variation (c.v.) of the expiratory interval.

Data are presented as means ± SD (n = 18–38 for each genotype). Asterisk indicates significantly different from wild-type mice, $p < 0.001$ (Student's t test).

lar breathing as recorded during periods without limb or body movements. Breathing patterns and respiratory frequencies were not significantly different between both genotypes (Figure 3C). In contrast, GlyT1$^{-/-}$ newborn animals displayed a severe depression of respiratory frequencies to 16% ($p < 0.001$) of those of wild-type pups (Figures 3B and 3C). The durations of single breaths were only marginally longer, but expiratory intervals were considerably prolonged. The irregularity of breathing was characterized by a 4-fold increase of the coefficient of variation ($p < 0.001$, Figure 3D) that again was not found in heterozygous littermates. In conclusion, GlyT1$^{-/-}$ animals showed a severe respiratory deficiency that may be causal for their early death.

### GlyT1$^{-/-}$ Mice Show Normal Histology and Synaptic Protein Expression

To reveal eventual developmental abnormalities in GlyT1$^{-/-}$ mice, a general histological analysis of cresyl violet-stained sections was performed. Both macroscopic organ sizes and morphologies at the light microscopic level were completely normal in all tissues examined, and no differences were detected between wild-type and GlyT$^{-/-}$ littermates (Figures 4A and 4B). Bronchioles displayed uniformly expanded alveolar ducts and alveoli, showing that respiratory depression in GlyT1$^{-/-}$ mutants was not due to malformations of the airways or lungs (Figures 4C and 4D). Similarly, no alterations of the musculo-skeletal system could be detected.

Since no anatomical changes of peripheral organs were found, systematic histological analysis of the CNS was performed. The corpus callosum of GlyT1$^{-/-}$ mice was fully developed as compared to control animals, and the hippocampi of the mutants contained a dentate gyrus and all CA pyramidal fields similar to those in wild-type mice (data not shown). Finally, brain stem and spinal cord sections of newborn GlyT1$^{-/-}$ mice did not differ morphologically from those of control littermates (Figures 4E–4H). Taken together, our data indicate that GlyT1$^{-/-}$ newborn animals were histologically indistinguishable from GlyT1$^{+/+}$ pups.

Different knockout experiments have shown that inactivation of a single gene may alter the expression of related proteins. Therefore, Western blot analyses were performed on pooled brain stem/spinal cord fractions prepared from wild-type, heterozygous, and homozygous GlyT1-deficient mice to determine whether expression levels of different synaptic components differed between these genotypes. Immunoblottings were carried out with antibodies against the $\alpha$ subunit of the GlyR (GlyR$\alpha$) (Pfeiffer et al., 1984); gephyrin, a postsynaptic protein involved in the clustering of glycine and $GABA_A$ receptors (Pfeiffer et al., 1984; Prior et al., 1992); the presynaptic vesicular inhibitory amino acid transporter (VIAAT), which transports glycine and GABA into synaptic vesicles (Dumoulin et al., 1999); GlyT2 (Liu et al., 1993); the NR1 subunit of the NMDA receptor (Moriyoshi et al., 1991); and the glial fibrillary acidic protein (GFAP) (Lewis et al., 1984). In all genotypes analyzed, the amounts of these proteins were not detectably altered (Figure 4I). Quantification of the immunreactive bands indicated that the rate of synthesis of these proteins did not change upon GlyT1 deficiency (Table 2).

In an attempt to verify whether inactivation of GlyT1 may cause adaptive changes in synapse densities, brain stem and spinal cord sections were stained with antibodies specific for the synaptic components described above (Figure 4J). No difference in the typical punctate staining, i.e., the synaptic localization, of GlyR$\alpha$ (Kirsch and Betz, 1995) was detected when comparing GlyT1$^{-/-}$ and control sections. Likewise, the density of gephyrin puncta indicative of inhibitory postsynaptic membrane specializations (Kneussel and Betz, 2000) was not altered in spinal cord sections of GlyT1$^{-/-}$ mice. By using antibodies against both VIAAT and GlyT2, the distribution of inhibitory presynaptic terminals was evaluated. Again, no changes in VIAAT (Dumoulin et al., 1999) and GlyT2 (Jursky and Nelson, 1995) punctate immunostaining were seen between GlyT1$^{-/-}$ mice and wild-type littermate sections. In addition, the integrity of glial cells was analyzed using antibodies against GFAP and GlyT1. In both wild-type and mutant mice, similar patterns of GFAP glial cell staining were obtained. Consistent with previous results (Zafra et al., 1995a), GlyT1 staining of wild-type sections revealed processes of glial cells that penetrated in between the perikarya of neurons and formed a dense network around dendrites and cell bodies (Figure 4J, and not shown). As expected, no GlyT1 staining was detected in preparations from homozygous mutants.

### GlyT1$^{-/-}$ Mice Show Abnormal In Vitro Respiratory Activity

As GlyT1$^{-/-}$ mice did not breathe properly, neuronal activity of the isolated respiratory network was analyzed in transversal slices from caudal medulla (Smith et al., 1991; Ramirez et al., 1996; Hülsmann et al., 2000; Richter and Spyer, 2001). This preparation preserves both the pre-Bötzinger complex, the region essential for the control of the respiratory rhythm, and the connections to the hypoglossal nucleus, thereby allowing us to monitor in vitro inspiratory activity. Under control conditions, preparations from wild-type animals showed a regular rhythmic bursting (Figure 5A) at a frequency of $0.22 \pm 0.08$ Hz (mean $\pm$ SD; $n = 8$; Figure 5B). Similar results were obtained with heterozygous GlyT1$^{+/-}$ mutant mice (frequency of $0.16 \pm 0.07$ Hz; $n = 8$). In contrast, preparations from GlyT1$^{-/-}$ animals revealed prolonged periods of inactivity (Figure 5A), and burst frequency was only $0.06 \pm 0.04$ Hz ($n = 10$; $p < 0.001$; Figure 5B) with variable interburst intervals (Figure 5C). Interestingly, the rhythmic activity recovered in slices from GlyT1$^{-/-}$ mice after application of the GlyR antagonist strychnine (Figure 5A). In the presence of 2 $\mu$M strychnine, burst activity increased 3.6-fold, leading to a frequency ($0.27 \pm 0.09$ Hz; $n = 5$; $p = 0.002$; Figure 5B) comparable to that seen under control conditions in wild-type mice. However, under all conditions examined, the activity of slices from GlyT1$^{-/-}$ mice was consistently more irregular than that of wild-type preparations. The coefficient of variation of the interburst interval was $0.36 \pm 0.15$ in wild-type and $0.88 \pm 0.24$ in GlyT1$^{-/-}$ mice. Upon strychnine application, this irregularity of the rhythm was only partially improved (coefficient of variation $0.76 \pm 0.32$, $n = 5$; Figure 5C). In preparations from wild-type animals, no significant changes in burst frequency and

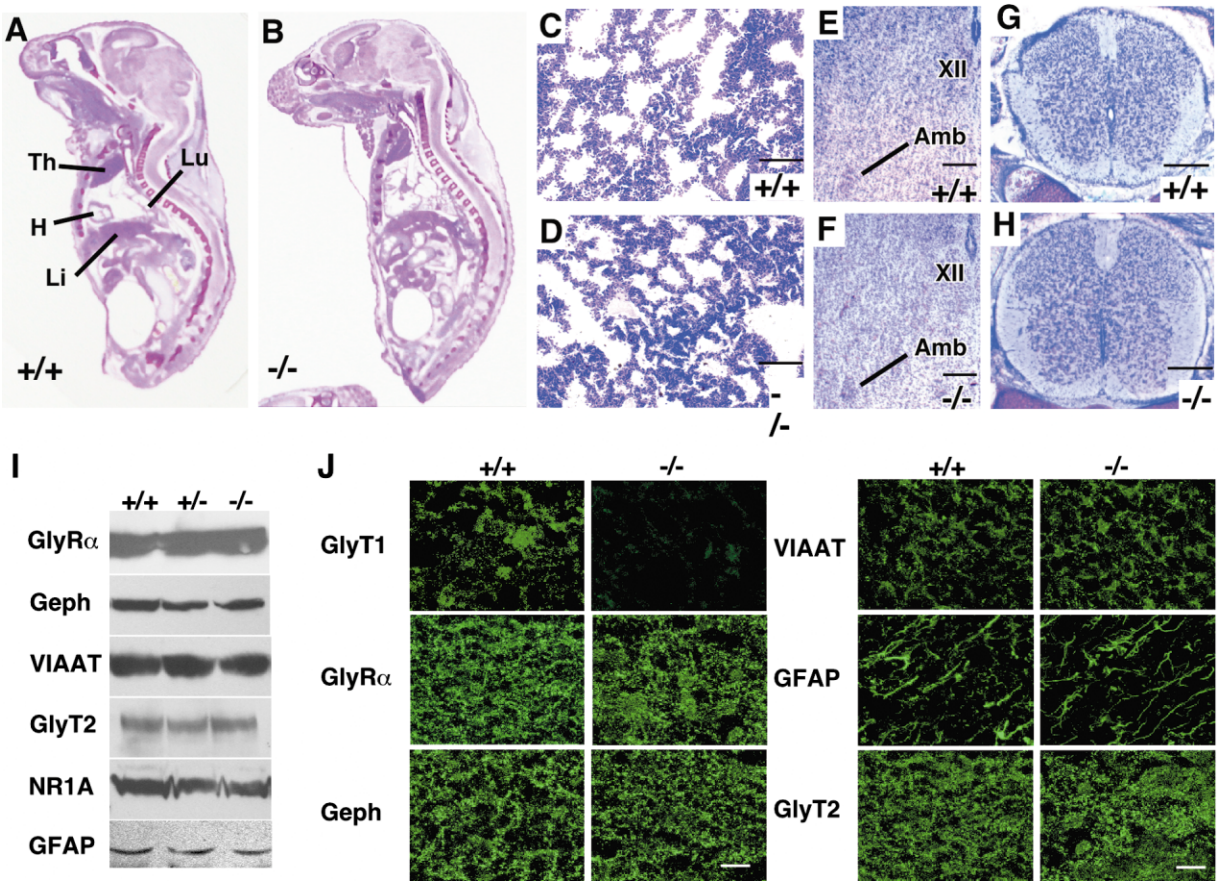


Figure 4. Histological and Immunochemical Analysis of GlyT1$^{-/-}$ Mice

(A–H) Cresyl violet-stained sections of wild-type (+/+) and GlyT1-deficient (−/−) mice. Sagital midline (A and B) and horizontal (C and D, scale bar equals 50 μm) sections are shown for wild-type (+/+) and GlyT1$^{-/-}$ mutant mice. No defects were detected, and the overall anatomy appeared normal for all animals analyzed. The corresponding sections of brain stem (E and F, scale bar equals 20 μm) and spinal cord (G and H, scale bar equals 100 μm) also revealed no alterations in the CNS structures of the homozygous mutants. XII, hypoglossal nucleus; Amb, nucleus ambiguus; Th, thymus; H, heart; Li, liver; Lu, lung.

(I) Western blot analysis of brain stem/spinal cord fractions prepared from newborn wild-type (+/+), heterozygous (+/−), and GlyT1 (−/−) mutant animals. Equal amounts of protein (40 μg/lane) were loaded and probed with the indicated antisera. Note that the expression levels of all proteins tested were not significantly different between genotypes.

(J) Immunohistochemistry of wild-type (+/+) and GlyT1$^{-/-}$ brain stem regions. Brain stem sections from newborn GlyT1$^{-/-}$ mice and wild-type littermates were stained with antibodies specific for the indicated proteins. Note that the punctate staining patterns of GlyRα, gephyrin, VIAAT, and GlyT2 seen in GlyT1$^{-/-}$ samples were indistinguishable from those in wild-type specimens. In addition, the density and morphology of glial cells stained for GFAP were unaltered in the mutants (scale bar equals 20 μm).

interburst interval were observed in the presence of strychnine. Also, no differences in rise time and burst duration were found between slices from wild-type and GlyT1$^{-/-}$ mice (Figures 5D and 5E). Notably, the application of the $GABA_A$ receptor antagonist bicuculline (1–2 μM) did not lead to a normalization of burst patterns (n = 3, data not shown).

Table 2. Quantification of Synaptic Protein Immunoreactivities

| Genotype | GlyT1$^{+/+}$ | GlyT1$^{+/-}$ | GlyT1$^{-/-}$ |
|---|---|---|---|
| GlyRα | 100± 17 | 98 ± 6 | 113 ± 9 |
| Gephyrin | 100 ± 15 | 91 ± 13 | 99.81 ± 17 |
| VIAAT | 100 ± 15 | 99 ± 18 | 108 ± 13 |
| GlyT2 | 100 ± 15 | 99 ± 13 | 114 ± 16 |
| NR1 | 100 ± 9 | 131 ± 22 | 120 ± 19 |
| GFAP | 100 ± 20 | 95 ± 22 | 103 ± 20 |

Values were determined by scanning immunoreactive bands on Western blots and represent means ± SD (n ≥ 3). None of the mutant values differs significantly from wild-type levels.

To more directly examine the effects of GlyT1 gene deletion on glycinergic transmission, whole-cell voltage-clamp recording was performed in hypoglossal motoneurons from wild-type and GlyT1$^{-/-}$ mice at a holding potential of −70 mV. Bicuculline (20 μM), CNQX (10 μM), and AP5 (100 μM) were added to the bath solution in order to block GABA and glutamate receptor-mediated transmission. The noise recorded from GlyT1$^{-/-}$ neurons was higher as compared to that from wild-type cells. During periods without obvious IPSCs, the average noise values (root-mean-square noise, rms) were 3.9 ± 0.8 pA (n = 5) in control and 8.3 ± 2.4 pA (n = 6, p = 0.003) in GlyT1$^{-/-}$ cells, respectively (Figures 6A and 6B). The mean interval of IPSCs identified in GlyT1$^{-/-}$

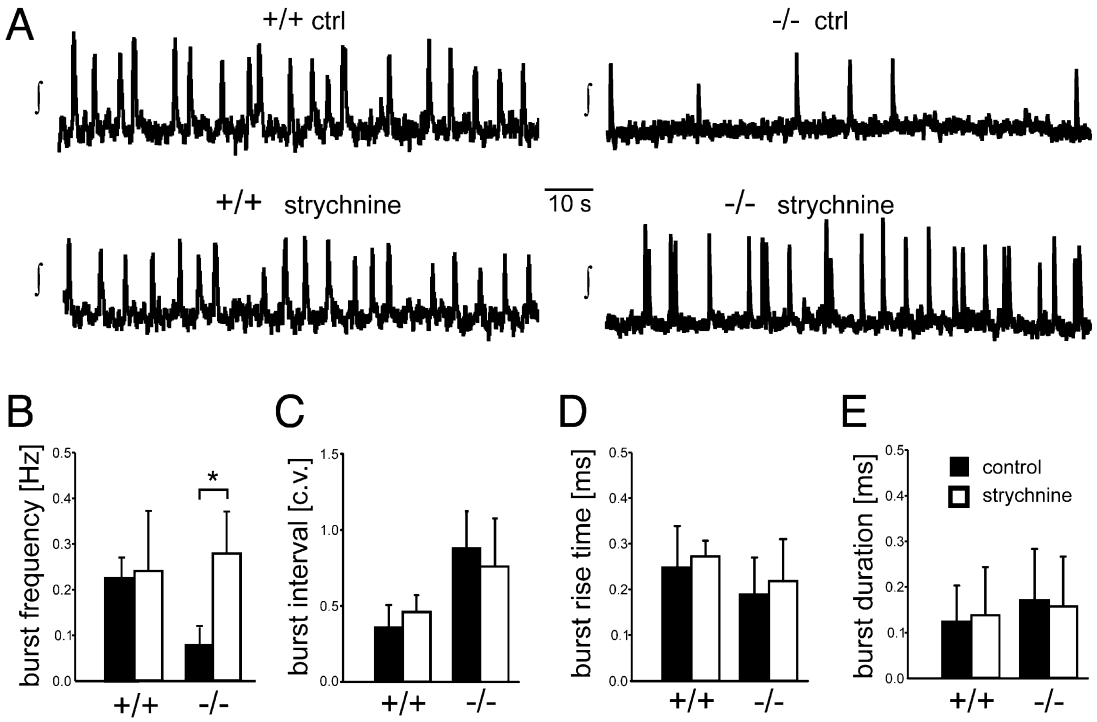


Figure 5. In Vitro Respiratory Activity in Brain Stem Slices of GlyT1$^{-/-}$ Mice

(A) Integrated network activities of slice preparations from newborn GlyT1$^{+/+}$ and GlyT1$^{-/-}$ mice. The GlyR antagonist strychnine (2 μM) did not increase breathing frequency in preparations from wild-type and heterozygous (not shown) mice, but normalized the respiratory frequency in slices from GlyT1$^{-/-}$ pups.

(B) In vitro burst frequencies (Hz) of wild-type and mutant animals as recorded under control conditions (black columns) and after application of strychnine (white columns).

(C) Regularity of in vitro respiratory bursting expressed by the coefficient of variation (c.v.) of the interburst interval, in the preparations shown in (B).

(D and E) Analysis of in vitro respiratory burst waveforms. (D) Rise (10%–90%) and (E) duration (half max amplitude) of inspiratory bursts (integrated activity) in slices from GlyT1$^{+/+}$ and in GlyT1$^{-/-}$ mice, prior to and after strychnine application.

Data in (B)–(E) are collected from recordings as shown in (A) and represent means ± SD ($n = 5$–10 for each genotype). Asterisk indicates significantly different, $p < 0.005$ (Student's t test).

neurons (1.7 ± 1.7 s, $n = 6$) was lower than in wild-type cells (8.6 ± 6.6 s, $n = 5$; $p = 0.03$; Figure 6C), whereas the averaged IPSC amplitude in GlyT1$^{-/-}$ neurons (46.1 ± 13.6 pA, $n = 6$) was not significantly smaller than in wild-type cells (51.4 ± 9.8 pA, $n = 5$; Figures 6D and 6E). In addition, the IPSC decay time was significantly prolonged upon GlyT1$^{-/-}$ deficiency (GlyT1$^{-/-}$, 14.2 ± 2.1 pA, $n = 6$; wild-type, 9.3 ± 0.6 pA, $n = 5$, $p = 0.001$; Figures 6F and 6G).

Application of strychnine reduced the steady-state holding current ($I_{hold}$) in identified hypoglossal motoneurons from GlyT1$^{-/-}$ animals ($\Delta I = 62.2$ pA; $p = 0.01$, $n = 4$), whereas no significant change was observed in preparations from wild-type mice (Figures 6A and 6H). Similarly, the increased synaptic noise seen in GlyT1$^{-/-}$ neurons was reduced to wild-type levels after application of strychnine (Figure 6B). Taken together, these data indicate that the suppression of respiratory network activity seen in GlyT1$^{-/-}$ mice is due to an increased accumulation of extracellular glycine, which leads to a sustained activation of inhibitory GlyRs.

Consistent with this interpretation, superfusion of wild-type slices with 1 mM glycine produced a strong suppression of in vitro respiratory activity to 3.2% of that seen under control conditions ($n = 3$, $p = 0.005$), which recovered upon washout (Figures 7A and 7B). Furthermore, application of the GlyT1-specific inhibitor sarcosine also produced a dose-dependent slowing of the rhythmic burst pattern in preparations from wild-type mice (Figures 7C and 7D). At a concentration of 2 mM, sarcosine reduced the network activity to 15.2% of wild-type values ($n = 4$, $p = 0.002$). Interestingly, no regular rhythm could be induced in slices from GlyT1$^{-/-}$ mice by application of the NMDA receptor blockers MK-801 and AP-5; even in the presence of both drugs, burst frequencies were unaltered (0.03 ± 0.04 Hz, $n = 3$; Figures 7E and 7F). These results imply that the depression of respiratory network activity is not due to increased NMDA receptor activity resulting from elevated glycine levels in the cerebrospinal fluid.

## Discussion

Here, we report a genetic analysis of the in vivo function of the glial GlyT subtype, GlyT1, in the mouse central nervous system. Inactivation of the GlyT1 gene by homologous recombination caused a complete loss of transporter expression, as demonstrated by Southern

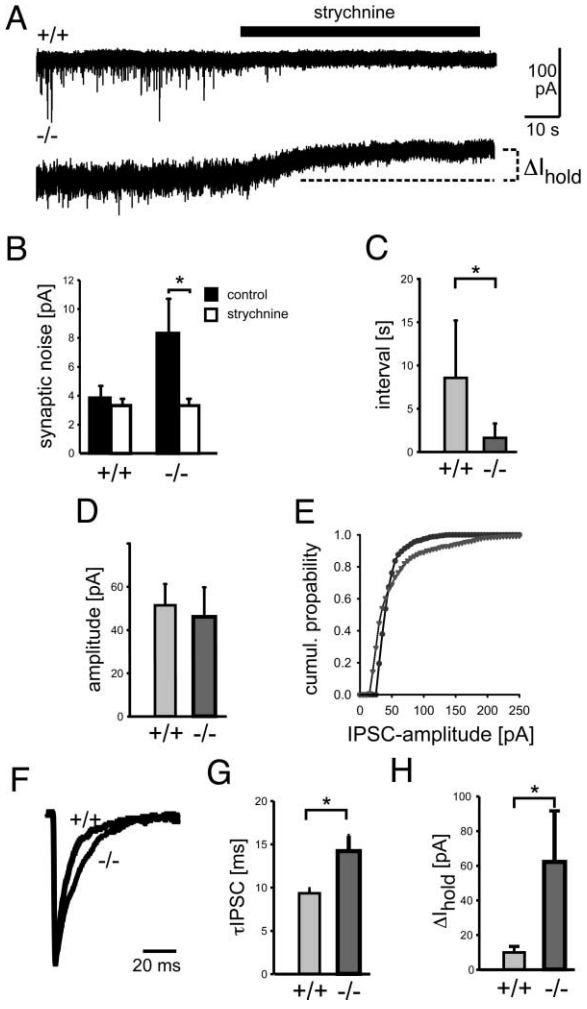


Figure 6. Whole-Cell Recordings from Hypoglossal Motoneurons

(A) Whole-cell currents of identified hypoglossal motoneurons recorded in the presence of 10 μM CNQX, 100 μM AP5, and 20 μM bicuculline. Application of the GlyR antagonist strychnine reduced the steady-state holding current in GlyT1$^{-/-}$ but not in GlyT1$^{+/+}$ animals.

(B) Synaptic noise recorded from hypoglossal motoneurons expressed as root-mean-square noise (rms) in GlyT1$^{+/+}$ and in GlyT1$^{-/-}$ mice. Note that synaptic noise in mutant mice (−/−) is reduced to wild-type level (c.f. Figure 7A) after application of strychnine (10 μM).

(C) Frequencies and mean amplitudes (D) of IPSCs recorded form hypoglossal motoneurons.

(E) Cumulative probability of spontaneous IPSC amplitudes (binned in 5 pA increments) in wild-type (triangles, 915 events, 5 cells) and GlyT1$^{-/-}$ (circles, 976 events, 6 cells) neurons recorded at 30°C. Note that events from GlyT1$^{-/-}$ neurons tend to have smaller amplitudes as evident from the leftward shift of the curve.

(F) Normalized and average waveforms of spontaneous IPSCs from hypoglossal motoneurons of GlyT1$^{+/+}$ and GlyT1$^{-/-}$ mice.

(G) Average decay times of identified spontaneous IPSCs from GlyT1$^{+/+}$ and GlyT1$^{-/-}$ mice.

(H) Average changes in steady-state holding current ($\Delta I_{hold}$) induced by the application of strychnine.

Data in (B)–(E), (G), and (H) are collected from recordings as shown in (A) and (F) and represent means ± SD (n = 4–6 for each genotype). Asterisk indicates significantly different.

blotting, RT-PCR, Western analysis, and [$^3$H]glycine uptake assays. Our data confirm the authenticity of the GlyT1$^{-/-}$ line and exclude the possibility that loss of GlyT1 may lead to compensatory changes in the expression of functionally closely related transporter proteins, e.g., the neuronal isoform GlyT2. The severe phenotype observed in the homozygous mutant mice thus can be confidently attributed to GlyT1 ablation.

### GlyT1 Has a Vital Role in the Postnatal CNS

Newborn GlyT1$^{-/-}$ pups consistently died during the first postnatal day, most likely due to respiratory failure combined with wasting and dehydration caused by the inability to suckle. Such early postnatal lethality has not been reported for other knockouts of related neurotransmitter transporters, e.g., dopamine transporter (Giros et al., 1996), serotonin transporter (Bengel et al., 1998), and norepinephrine transporter (Xu et al., 2000) deficient mice, but often is found upon inactivation of genes encoding proteins of glycinergic synapses. For example, gephyrin-deficient mice also die during the first postnatal day (Feng et al., 1998), whereas inactivation of the GlyR α1 subunit gene by a spontaneously generated microdeletion in the mouse mutant *oscillator* results in death during the third postnatal week (Buckwalter et al., 1994). A lethal phenotype resembling that of *oscillator* mice is also found in GlyT2-deficient animals (Gomeza et al., 2003). Together, these gene-targeting data emphasize the importance of glycinergic inhibition for proper functioning of the mammalian CNS.

The phenotype of GlyT1$^{-/-}$ mice cannot be attributed to insufficient differentiation or anatomical malformation. In contrast to observations made with other mouse mutants displaying a phenotypically similar early lethality (Forrest et al., 1994; Li et al., 1994; Hubner et al., 2001; Zhao et al., 2001), we did not detect any morphological defects in peripheral organs of GlyT1$^{-/-}$ newborn animals. Likewise, no histological abnormalities were found in sections of brain stem and spinal cord of mutant neonates at both light (this study) and electron (J.G. and K.O., unpublished results) microscopic levels. Thus, GlyT1 appears not to be required for organogenesis during embryonic development but is essential for vital postnatal CNS functions.

A surprising result obtained here is that ablation of the GlyT1 gene apparently does not lead to major adaptive alterations in synapse biochemistry. Previous studies with dopamine transporter, serotonin transporter, and norepinephrine transporter knockout mice have highlighted the importance of these transporters in modulating the extracellular dynamics of monoamines as well as in controlling pre- and/or postsynaptic protein expression, as revealed by up- or downregulation of specific components of the respective synapses (Bengel et al., 1998; Gainetdinov et al., 1998; Jones et al., 1998, 1999; Xu et al., 2000). In contrast, our Western blot analyses indicate similar expression levels of the GlyR α subunit, the NMDA receptor subunit NR1, gephyrin, VIAAT, and GlyT2 in all genotypes analyzed. Moreover, our immunohistochemical data show that the localization of different pre- and postsynaptic proteins of inhibitory synapses is unaltered in homozygous mutant animals. These results suggest that no major changes in synaptic

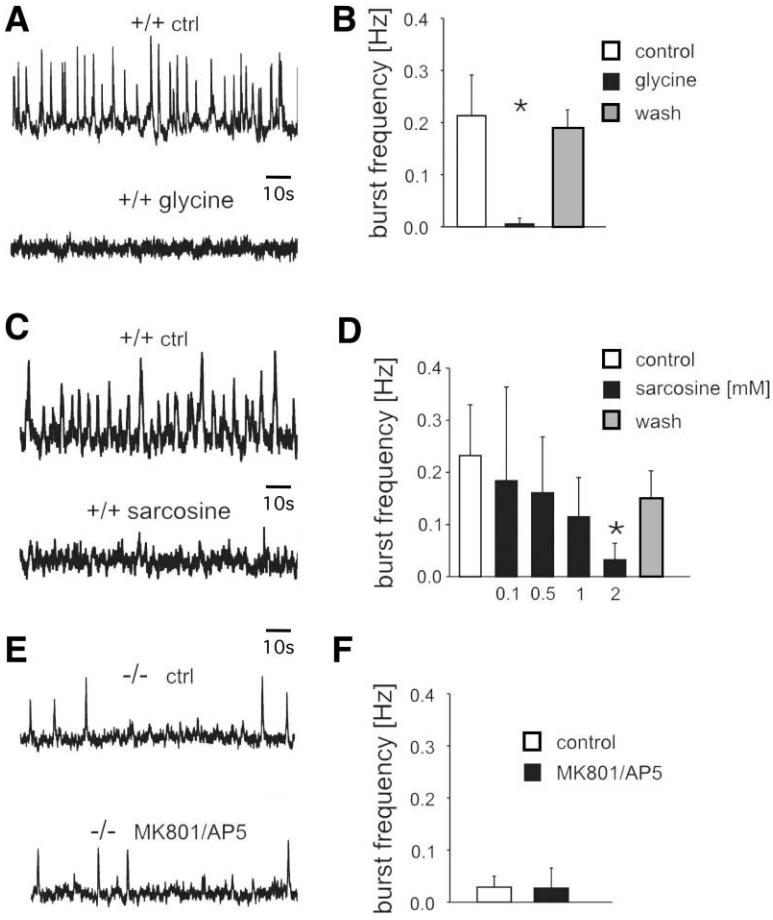


Figure 7. Effects of Glycine, Sarcosine, and NMDA Antagonists on In Vitro Respiration

(A) Response to the application of glycine (1 mM) is shown. In vitro respiratory activity is reversibly suppressed in brainstem slices from wild-type mice (+/+).

(B) Corresponding average burst frequencies.

(C) Dose-dependent inhibition of in vitro respiratory activity was also obtained by addition of the GlyT1 inhibitor sarcosine (2 mM).

(D) Dose dependence of respiratory suppression upon application of increasing concentrations of sarcosine as monitored by determination of burst frequencies as shown in (C).

(E) Application of the NMDA receptor blockers MK-801 (10 μM) and AP-5 (100 μM) did not restore a regular respiratory rhythm in slices from GlyT1-deficient mice (−/−).

(F) Average burst frequencies corresponding to (E).

Data are presented as means ± SD (n = 3–4 for each genotype). Asterisk indicates significantly different from control conditions, $p \leq 0.005$ (Student's t test).

protein accumulation occur in the CNS in response to inactivation of the GlyT1 gene. In addition, neither the expression level of GFAP, a glial marker protein (Lewis et al., 1984), nor glial cell morphology were altered in the GlyT1$^{-/-}$ mice. Thus, the respiratory deficiency seen in the mutants cannot be attributed to glial cell death. In conclusion, all presently available data suggest that neuronal, glial, and synaptic differentiation proceed normally in GlyT1-deficient embryos. Similarly, in mice lacking GlyT2, synaptic differentiation is not affected (Gomeza et al., 2003).

### GlyT1 Is Essential for Lowering Glycine Concentrations at Inhibitory GlyRs

One of the crucial roles of GlyT1 clearly lies in the regulation of centrally generated rhythmic motor functions that are essential for autonomous neonatal life, such as breathing. Our recordings of in vivo breathing behavior on the first postnatal day indicate a dramatic depression of respiratory frequency in the homozygous mutants. Instead of the regular breathing characteristic of wild-type animals, gasp-like inspirations interrupted long periods of apnea in GlyT1$^{-/-}$ pups. This points to an important role of glycine uptake by glial cells in the control of respiratory rhythms in newborn animals.

Although the failure of strychnine application to alter respiratory activity in slice preparations from newborn rodents has led to the postulate that glycinergic inhibition is not essential for the generation of the respiratory rhythm in newborn mice (Paton et al., 1994; Ramirez et al., 1996), our analysis of in vivo breathing behavior and in vitro network activity indicate a dramatic depression of respiratory activity in GlyT1$^{-/-}$ neonates. This is consistent with enhanced inhibition caused by the accumulation of extracellular glycine in the mutant animals. We are aware of the fact that there is an ongoing debate whether chloride-mediated inhibition by glycine or GABA is functional immediately after birth. Data from respiratory neurons (Ritter and Zhang, 2000) and hypoglossal motoneurons (Singer et al., 1998) have suggested that the choride equilibrium potential is depolarizing in neonatal mice. This might explain why transient activation of GlyRs does not influence respiratory network activity in wild-type mice (Paton et al., 1994; Zhang et al., 2002). Persistent GlyR activation by excess glycine, however, will cause inhibition and depression of network activity through shunting of neuronal input resistance. Therefore, the crucial consequences of GlyT1 deletion most likely result from insufficient regulation of extracellular levels of glycine at GlyRs of respiratory neurons.

While respiratory rhythm generation can be attributed to the neuronal network in the pre-Bötzinger complex (Smith et al., 1991; Ramirez et al., 1996; Richter and Spyer, 2001), glial cells have been postulated to exert a modulatory and stabilizing function. Previous pharmacological studies have shown that metabolic coupling

between glia and neurons is necessary for maintaining rhythmic activity in the respiratory network (Hülsmann et al., 2000). Our in vitro data from rhythmic slices of newborn wild-type and GlyT1$^{-/-}$ animals extend these findings. The reduction of spontaneous activity in GlyT1$^{-/-}$ preparations provides direct genetic proof that glial glycine uptake by GlyT1 is essential for stabilizing respiratory network activity. Furthermore, glycine and the GlyT1 inhibitor sarcosine induced a slowing of the rhythmic burst pattern in wild-type slices, which mimicked that seen in GlyT1$^{-/-}$ mice, suggesting that ablation of GlyT1 function does not lead to alterations in cellular, synaptic, or network architecture. In addition, the normalization of firing frequency seen in the GlyT1$^{-/-}$ but not wild-type slices upon application of the GlyR antagonist strychnine is consistent with extracellular levels of glycine being elevated in mutant as compared to wild-type animals. Taken together, our results demonstrate that during early postnatal life GlyT1 modulates the activation of GlyRs in caudal regions of the CNS.

Depending on physiological conditions, GlyT1-mediated glycine uptake into or release from glial cells (Roux and Supplisson, 2000) could result in suppression or potentiation of NMDA receptor function. However, this hypothesis could not be directly tested in our slice preparations, since NMDA receptor blockers did not restore regular rhythmicity of in vitro respiration in GlyT1$^{-/-}$ preparations. Similarly, NMDA receptor antagonists have been reported to have no or only minor effects on in vitro respiration in slices from neonatal rats (Greer et al., 1991; Funk et al., 1993). Further evidence against a significant role of NMDA receptors in post-partum respiratory control comes from electrophysiological studies with mutant mice lacking the essential NMDA receptor subunit NR1 (Funk et al., 1997). In these experiments, brain stem-medullary slice preparations from homozygous NR1-deficient mutants generated a respiratory rhythm virtually identical to that in wild-type, although the NMDA receptor-mediated modulation of the respiratory rhythm is impaired. Thus, NMDA receptors are not essential for respiratory rhythm generation in the neonate. It should, however, be emphasized that our results do not exclude an important role of GlyT1 in the regulation of NMDA receptor activation by glutamate in other regions of the central nervous system or at later developmental stages. Notably, a very recent study indicates that increased levels of glycine cause internalization of NMDA receptors by clathrin-mediated endocytosis (Nong et al., 2003). Such coagonist-triggered downregulation of NMDA receptors might explain the inability of strychnine to fully restore all parameters of the in vitro respiration in slice preparations from GlyT1$^{-/-}$ mice. In addition, GlyT1 may have a role in regulating the activity of excitatory glycine receptors that may form by the assembly of the NMDA receptor NR1 and NR3 subunits (Chatterton et al., 2002).

### GlyT1$^{-/-}$ Mice as a New Animal Model of the Human Glycine Encephalopathy Syndrome

As outlined above, during neonatal life GlyT1 appears to be the major GlyT isoform that catalyzes the clearance of extracellular glycine in caudal regions of the CNS, since its inactivation is not functionally compensated by the neuronally expressed GlyT2 protein. GlyT1$^{-/-}$ mice display severe motor deficits accompanied by lethargy, hypotonia, and hyporesponsivity. This overall reduction of motosensory functions is similar to some of the symptoms associated with a group of inherited human diseases that develop in early postnatal life, named glycine encephalopathy or nonketotic hyperglycinemia (NKH). Muscular hypotonia, lethargy, and poor feeding with hiccups characterize these disorders (Tada et al., 1992; Boneh et al., 1996; Lu et al., 1999; Applegarth and Toone, 2001). NKH can rapidly progress to a lethal symptomatology with respiratory insufficiency, apnea, coma, and finally death. Enzymatic analysis indicates that most patients with NKH have a primary defect in the glycine cleavage system that degrades excess intracellular glycine (Boneh et al., 1996; Applegarth and Toone, 2001). As a consequence, elevated levels of glycine accumulate in the blood and cerebrospinal fluid of the affected individuals. Notably, in the CNS the glycine cleavage system is localized in astrocytic glial cells where it is thought to metabolize glycine provided by GlyT1-mediated uptake (Sato et al., 1991; Sakata et al., 2001). Thus, some yet unclassified forms of NKH might involve mutations in the GlyT1 gene, since reduced glial glycine uptake similarly will result in elevated cerebrospinal glycine levels. Indeed, a 20-year-old study describes an atypical case of NKH with a defective glycine transport system in postmortem nervous tissue (Mayor et al., 1984). It should be emphasized that such mutations may not cause the full range of classical NKH symptoms, as several symptoms are directly linked to the loss of glycine cleavage activity (Applegarth and Toone, 2001). In conclusion, our GlyT1-deficient mice might provide a useful animal model to study the pathomechanisms of glycine encephalopathy.

## Experimental Procedures

### Generation of GlyT1$^{-/-}$ Mice

The mouse gene encoding GlyT1 was isolated from a mouse genomic library prepared from 129SvJ mouse DNA (Genome Systems, St. Louis, MO) by hybridization with a PCR fragment corresponding to the region of the GlyT1 cDNA that encodes the middle of the fourth up to the sixth transmembrane domain. The targeting vector consisted of a 5.9 kb genomic sequence, including exons 1c to 4, in which a 0.37 kb fragment encompassing exon 3 was replaced with the 1.8 kb PGK-neomycin resistance gene (PGK-neo). A 2.8 kb herpex simplex virus thymidine kinase gene fragment was attached to the 3′ end of the construct for negative selection. The targeting vector was linearized at a unique NotI site and introduced into E14 (129/OLA) mouse embryonic stem (ES) cells by electroporation, followed by selection in G418 and FIAU. Colonies that survived the double selection procedure were isolated and screened by Southern blotting for homologous recombination using a 3′ external probe. This analysis showed that 2 out of a total of 136 screened clones had been targeted properly. Positive ES cell clones were injected into C57BL/6 blastocysts to generate chimeras that were backcrossed with female C57BL/6 mice. Heterozygous offspring were crossed to yield homozygous mutant animals. All mice used in the present study were F2 hybrids.

### RNA Isolation and RT-PCR Analysis

Total RNA was obtained from brain stem and spinal cord preparations of each genotype as described (Chomczynski and Sacchi, 1987). For comparative RT-PCR analyses, the following sense (s) and antisense (as) primers were used: GlyT1, OL-5 (s) 5′-AACTGGG GCAACCAGATCGA-3′ (transmembrane domain TM1) and OL-102

(as) 5′-GTACATGATACCCGTGAAGGC (TM5), both oligos flanking the selection marker cassette and yielding a 735 bp fragment; GlyT2, Ol-201 (s) 5′-TCTGCAGGGATTGAATATCC-3′ and OL-303 (as) 5′-CTC AATGTTGACTTTGCGCTC-3′, generating a 460 bp fragment; β-actin, OL-ActinS (s) 5′-ATACCAACCGTGAAAAGATGA-3′ and OL-Actin-AS1 (as) 5′-ATACCCAAGAAGGAAGGCTGG-3′, yielding a 469 bp PCR band.

The reactions were carried out according to standard protocols (Kawasaki, 1990). Tubes contained equal aliquots of RNA for RT reactions. PCR amplification was done by an initial denaturation at 94°C for 10 min and 30 cycles of denaturation (94°C, 30 s), annealing (55°C, 30 s), and extension (72°C, 1 min).

### Brain Membrane Preparation

Mouse brain samples were homogenized in 1 ml of ice-cold isolation medium (0.33 M sucrose, 1 mM EDTA, 1 mM phenylmethylsulfonyl fluoride, 10 mM HEPES-Tris [pH 7.4]) using a Dounce-type glass homogenizer. The homogenate was centrifuged (1000 × g, 5 min) at 4°C, the pellet discarded, and the supernatant centrifuged at 17,000 × g for 10 min. The resulting high-speed pellet (P2) was washed once and resuspended in modified Krebs-Henseleit medium (125 mM NaCl, 5 mM KCl, 2.7 mM $CaCl_2$, 1.3 mM $MgSO_4$, 10 mM glucose, 25 mM HEPES-Tris [pH 7.4]). Protein concentrations were determined using a protein assay system (Bio-Rad, München, Germany).

### [$^3$H]Glycine Transport Assay

20 μl aliquots of the membrane suspension (equivalent to 30–50 μg of protein) were preincubated for 2 min at 37°C. Uptake was initiated by addition of 80 μl of a modified Krebs-Henseleit solution kept at 37°C containing [2-$^3$H]glycine (2 μM) (1.52 GBq/μmol, Movasek Biochemicals, Brea, CA). After a 1 min incubation with gentle agitation, uptake was terminated by diluting the incubation mixture with 3 ml of modified Krebs-Henseleit medium kept at room temperature followed by rapid filtration through a moistened filter (SM 11106, 0.45 μm pore size) (Sartorius, Göttingen, Germany). Filters were rinsed twice with 3 ml of modified Krebs-Henseleit medium. All dilution, filtration, and washing procedures were performed within 15 s. Filters were dried and placed in microvials, and their radioactivity measured by scintillation spectrometry.

### Western Blotting

Crude membrane fractions prepared from mouse brain stem and spinal cord (40 μg of protein) were separated by 8% SDS-polyacrylamide gel electrophoresis, transferred to nitrocellulose (Schleicher & Schüll, Dassel, Germany), and probed with antibodies specific for GlyT1 (1:3000) (kindly provided by Carmen Aragon and Francisco Zafra), gephyrin (Pfeiffer et al., 1984; Prior et al., 1992) (1:500), VIAAT (1:1000) (kindly provided by Bruno Gasnier), GlyT2 (1:1000), the α subunit of the GlyR (Pfeiffer et al., 1984) (1:1000), and the NR1A subunit of the NMDA receptor (1:500) (Chemicon, Hofheim, Germany). After washing, bound Igs were visualized with horseradish peroxidase-conjugated secondary antibodies using the ECL detection system (Pierce, Rockford, IL). The Western blots were scanned and digitalized images were analyzed for quantification using the software NIH-Image 1.63.

### Histology and Immunocytochemistry

Histological and immunocytochemical analysis was performed on GlyT1$^{+/+}$ and GlyT1$^{-/-}$ neonates (>3 animals per genotype). The pups were anesthesized, frozen, and cut into 20 μm sections on the cryostat. Sections were fixed with 4% (w/v) paraformaldehyde in standard PBS (pH 7.4) and stained with 0.1% (w/v) cresyl violet. For immunostaining, 12 μm cryostat sections were cut and immediately fixed with 4% (w/v) paraformaldehyde for 2 min, washed in PBS, and incubated with primary and secondary antibodies as described (Kirsch and Betz, 1995; Feng et al., 1998). Confocal microscopy was performed using a confocal laser-scanning microscope (Leica) equipped with the image software Leica TCS-NT.

### Respiratory Network Analysis

Plethysmographic measurements were performed at room temperature using a 10 ml whole-body plethysmographic chamber. Pressure fluctuations were measured with a differential low-pressure transducer (model DP103, Validyne Engineering, Northridge, CA) connected to a sine wave carrier demodulator (CD-15). Breathing movements were monitored for 3 min during the first 12–14 hr after birth. Artifacts originating from spontaneous limb movements were excluded from analysis.

In vitro respiratory activity of isolated brainstem slice preparations, containing the intact pre-Bötzinger complex and the synaptically connected hypoglossal nucleus, was monitored from hypoglossal rootlets or from the slice surface that exposed the pre-Bötzinger complex. Preparation and recording techniques were as described before (Ramirez et al., 1996; Hülsmann et al., 2000). Slices, 600–750 μm thick, were superfused with artificial spinal fluid (ACSF) at 30°C gassed with 95% $O_2$/5% $CO_2$. ACSF contained (in mM): 118 NaCl, 8 KCl, 1.5 $CaCl_2$, 1 $MgCl_2$, 1 $NaH_2P0_4$, 25 $NaHCO_3$, and 30 D-glucose (pH 7.4, 310 mosmol/l). Respiration-related burst discharges were amplified by a custom-made differential amplifier, filtered, rectified, and then integrated. Respiratory frequencies were calculated as the reciprocal values of the mean expiratory interval.

### Whole-Cell Voltage-Clamp Experiments

Microelectrodes were pulled from borosilicate glass capillary tubings (Biomedical Instruments, Germany) and had resistances ranging between 5 and 7 MΩ. The electrode solution contained (in mM) 125 KCl, 1 $CaCl_2$, 10 1,2-bis(2-aminophenoxy)-ethane-N,N,N′,N′-tetraacetic acid (BAPTA), 2 $MgCl_2$, 4 $Na_2ATP$, 10 N-2-hydroxyethylpiperazine-N′-2-ethanesulfonic acid (HEPES) (pH adjusted to 7.2 with KOH). Under these conditions, the equilibrium potential for chloride was about 0 mV. Therefore, at a holding potential of −70 mV we observed glycinergic IPSCs as inward currents. Currents were recorded using a Multiclamp 700 patch-clamp amplifier (Axon Instruments Inc., Foster City, CA), low-pass filtered at 3 kHz, and sampled at 10 kHz and analyzed on a PC using an interface (Digidata1320) and pClamp 8.2 software (Axon Instruments). Series resistance and cell membrane capacitance were compensated prior to recordings. Synaptical events were analyzed by using Mini Analysis Program (Synaptosoft, Leonia, NY), which allows for threshold-based event detection. Frequencies and amplitudes of spontaneous IPSCs were determined from 2–3 min epochs recordings, by using the software event detector set to identify events above background. IPSC events were visually inspected to ensure that no false IPSCs were included in data sets. For calculation of the time constants of IPSC decay, IPSCs that were 8–10 times larger than the noise level were detected by the program; double-peak IPSCs were excluded from analysis. Spontaneous IPSC decay phases were fit by two exponentials, and the mean time constant, $t_{decay}$, was calculated from the respective time constants and their relative amplitudes: $t_{decay} = t_1a_1/t_2a_2$ using the Mini Analysis Program.

### Acknowledgments

This work was supported by Deutsche Forschungsgemeinschaft (SFB 296/A1 and SFB 406/C10), European Community (TMR ERBFMRXCT9), Bundesministerium für Bildung und Forschung (01KV0002), State of Lower Saxony (Lichtenberg Stipend to K.S.), and Fonds der Chemischen Industrie. We thank Belquis Rahim, Dagmar Magalei, and Anja-Annett Grützner for technical assistance, John Caldwell for critical reading, and Maren Baier for help with preparation of the manuscript.

Received: February 24, 2003
Revised: July 10, 2003
Accepted: September 29, 2003
Published: November 12, 2003

### References

Adams, R.H., Sato, K., Shimada, S., Tohyama, M., Puschel, A.W., and Betz, H. (1995). Gene structure and glial expression of the glycine transporter GlyT1 in embryonic and adult rodents. J. Neurosci. *15*, 2524–2532.

Amara, S.G., and Kuhar, M.J. (1993). Neurotransmitter transporters: recent progress. Annu. Rev. Neurosci. *16*, 73–93.

Applegarth, D.A., and Toone, J.R. (2001). Nonketotic hyperglycinemia (glycine encephalopathy): laboratory diagnosis. Mol. Genet. Metab. *74*, 139–146.

Bengel, D., Murphy, D.L., Andrews, A.M., Wichems, C.H., Feltner, D., Heils, A., Mossner, R., Westphal, H., and Lesch, K.P. (1998). Altered brain serotonin homeostasis and locomotor insensitivity to *3*, 4-methylenedioxymethamphetamine ("Ecstasy") in serotonin transporter-deficient mice. Mol. Pharmacol. *53*, 649–655.

Berger, A.J., Dieudonne, S., and Ascher, P. (1998). Glycine uptake governs glycine site occupancy at NMDA receptors of excitatory synapses. J. Neurophysiol. *80*, 3336–3340.

Betz, H., Harvey, R.J., and Schloss, P. (2000). Structures, diversity and pharmacology of glycine receptors and transporters. In Pharmacology of GABA and Glycine Neurotransmission, H. Möhler, ed. (Berlin: Springer-Verlag), pp. 375–401.

Boneh, A., Degani, Y., and Harari, M. (1996). Prognostic clues and outcome of early treatment of nonketotic hyperglycinemia. Pediatr. Neurol. *15*, 137–141.

Buckwalter, M.S., Cook, S.A., Davisson, M.T., White, W.F., and Camper, S.A. (1994). A frameshift mutation in the mouse alpha 1 glycine receptor gene (Glra1) results in progressive neurological symptoms and juvenile death. Hum. Mol. Genet. *3*, 2025–2030.

Chatonnet, F., del Toro, E.D., Voiculescu, O., Charnay, P., and Champagnat, J. (2002). Different respiratory control systems are affected in homozygous and heterozygous kreisler mutant mice. Eur. J. Neurosci. *15*, 684–692.

Chatterton, J.E., Awobuluyi, M., Premkumar, L.S., Takahashi, H., Talantova, M., Shin, Y., Cui, J., Tu, S., Sevarino, K.A., Nakanishi, N., et al. (2002). Excitatory glycine receptors containing the NR3 family of NMDA receptor subunits. Nature *415*, 793–798.

Chomczynski, P., and Sacchi, N. (1987). Single-step method of RNA isolation by acid guanidinium thiocyanate-phenol-chloroform extraction. Anal. Biochem. *162*, 156–159.

Dumoulin, A., Rostaing, P., Bedet, C., Levi, S., Isambert, M.F., Henry, J.P., Triller, A., and Gasnier, B. (1999). Presence of the vesicular inhibitory amino acid transporter in GABAergic and glycinergic synaptic terminal boutons. J. Cell Sci. *112*, 811–823.

Feng, G., Tintrup, H., Kirsch, J., Nichol, M.C., Kuhse, J., Betz, H., and Sanes, J.R. (1998). Dual requirement for gephyrin in glycine receptor clustering and molybdoenzyme activity. Science *282*, 1321–1324.

Forrest, D., Yuzaki, M., Soares, H.D., Ng, L., Luk, D.C., Sheng, M., Stewart, C.L., Morgan, J.I., Connor, J.A., and Curran, T. (1994). Targeted disruption of NMDA receptor 1 gene abolishes NMDA response and results in neonatal death. Neuron *13*, 325–338.

Fortin, G., Foutz, A.S., and Champagnat, J. (1994). Respiratory rhythm generation in chick hindbrain: effects of MK-801 and vagotomy. Neuroreport *5*, 1137–1140.

Friauf, E., Aragon, C., Lohrke, S., Westenfelder, B., and Zafra, F. (1999). Developmental expression of the glycine transporter GLYT2 in the auditory system of rats suggests involvement in synapse maturation. J. Comp. Neurol. *412*, 17–37.

Funk, G.D., Smith, J.C., and Feldman, J.L. (1993). Generation and transmission of respiratory oscillations in medullary slices: role of excitatory amino acids. J. Neurophysiol. *70*, 1497–1515.

Funk, G.D., Johnson, S.M., Smith, J.C., Dong, X.W., Lai, J., and Feldman, J.L. (1997). Functional respiratory rhythm generating networks in neonatal mice lacking NMDAR1 gene. J. Neurophysiol. *78*, 1414–1420.

Gainetdinov, R.R., Jones, S.R., Fumagalli, F., Wightman, R.M., and Caron, M.G. (1998). Re-evaluation of the role of the dopamine transporter in dopamine system homeostasis. Brain Res. Brain Res. Rev. *26*, 148–153.

Giros, B., Jaber, M., Jones, S.R., Wightman, R.M., and Caron, M.G. (1996). Hyperlocomotion and indifference to cocaine and amphetamine in mice lacking the dopamine transporter. Nature *379*, 606–612.

Gomeza, J., Ohno, K., Hulsmann, S., Armsen, W., Eulenburg, V., Richter, D.W., Laube, B., and Betz, H. (2003). Deletion of the mouse glycine transporter 2 results in a hyperekplexia phenotype and postnatal lethality. Neuron *40*, this issue, 797–806.

Greer, J.J., Smith, J.C., and Feldman, J.L. (1991). Role of excitatory amino acids in the generation and transmission of respiratory drive in neonatal rat. J. Physiol. *437*, 727–749.

Guastella, J., Brecha, N., Weigmann, C., Lester, H.A., and Davidson, N. (1992). Cloning, expression, and localization of a rat brain high-affinity glycine transporter. Proc. Natl. Acad. Sci. USA *89*, 7189–7193.

Hubner, C.A., Stein, V., Hermans-Borgmeyer, I., Meyer, T., Ballanyi, K., and Jentsch, T.J. (2001). Disruption of KCC2 reveals an essential role of K-Cl cotransport already in early synaptic inhibition. Neuron *30*, 515–524.

Hülsmann, S., Oku, Y., Zhang, W., and Richter, D.W. (2000). Metabolic coupling between glia and neurons is necessary for maintaining respiratory activity in transverse medullary slices of neonatal mouse. Eur. J. Neurosci. *12*, 856–862.

Johnson, J.W., and Ascher, P. (1987). Glycine potentiates the NMDA response in cultured mouse brain neurons. Nature *325*, 529–531.

Johnston, G.A., and Iversen, L.L. (1971). Glycine uptake in rat central nervous system slices and homogenates: evidence for different uptake systems in spinal cord and cerebral cortex. J. Neurochem. *18*, 1951–1961.

Jones, S.R., Gainetdinov, R.R., Jaber, M., Giros, B., Wightman, R.M., and Caron, M.G. (1998). Profound neuronal plasticity in response to inactivation of the dopamine transporter. Proc. Natl. Acad. Sci. USA *95*, 4029–4034.

Jones, S.R., Gainetdinov, R.R., Hu, X.T., Cooper, D.C., Wightman, R.M., White, F.J., and Caron, M.G. (1999). Loss of autoreceptor functions in mice lacking the dopamine transporter. Nat. Neurosci. *2*, 649–655.

Jursky, F., and Nelson, N. (1995). Localization of glycine neurotransmitter transporter (GLYT2) reveals correlation with the distribution of glycine receptor. J. Neurochem. *64*, 1026–1033.

Kawasaki, E.S. (1990). Amplification of RNA. In PCR Protocols, M.A. Innis, D.H. Gelfand, J.J. Sninsky, and T.J. White, eds. (San Diego, CA:4 Academic Press), pp. 21–27.

Kirsch, J., and Betz, H. (1995). The postsynaptic localization of the glycine receptor-associated protein gephyrin is regulated by the cytoskeleton. J. Neurosci. *15*, 4148–4156.

Kneussel, M., and Betz, H. (2000). Clustering of inhibitory neurotransmitter receptors at developing postsynaptic sites: the membrane activation model. Trends Neurosci. *23*, 429–435.

Legendre, P. (2001). The glycinergic inhibitory synapse. Cell. Mol. Life Sci. *58*, 760–793.

Lewis, S.A., Balcarek, J.M., Krek, V., Shelanski, M., and Cowan, N.J. (1984). Sequence of a cDNA clone encoding mouse glial fibrillary acidic protein: structural conservation of intermediate filaments. Proc. Natl. Acad. Sci. USA *81*, 2743–2746.

Li, Y., Erzurumlu, R.S., Chen, C., Jhaveri, S., and Tonegawa, S. (1994). Whisker-related neuronal patterns fail to develop in the trigeminal brainstem nuclei of NMDAR1 knockout mice. Cell *76*, 427–437.

Liu, Q.R., Nelson, H., Mandiyan, S., Lopez-Corcuera, B., and Nelson, N. (1992). Cloning and expression of a glycine transporter from mouse brain. FEBS Lett. *305*, 110–114.

Liu, Q.R., Lopez-Corcuera, B., Mandiyan, S., Nelson, H., and Nelson, N. (1993). Cloning and expression of a spinal cord- and brain-specific glycine transporter with novel structural features. J. Biol. Chem. *268*, 22802–22808.

Lopez-Corcuera, B., Geerlings, A., and Aragon, C. (2001). Glycine neurotransmitter transporters: an update. Mol. Membr. Biol. *18*, 13–20.

Lu, F.L., Wang, P.J., Hwu, W.L., Tsou Yau, K.I., and Wang, T.R. (1999). Neonatal type of nonketotic hyperglycinemia. Pediatr. Neurol. *20*, 295–300.

Mayor, F., Jr., Martin, A., Rodriguez-Pombo, P., Garcia, M.J., Benavides, J., and Ugarte, M. (1984). Atypical nonketotic hyperglycinemia

with a defective glycine transport system in nervous tissue. Neurochem. Pathol. *2*, 233–249.

Moriyoshi, K., Masu, M., Ishii, T., Shigemoto, R., Mizuno, N., and Nakanishi, S. (1991). Molecular cloning and characterization of the rat NMDA receptor. Nature *354*, 31–37.

Nelson, N. (1998). The family of $Na^+/Cl^-$ neurotransmitter transporters. J. Neurochem. *71*, 1785–1803.

Nong, Y., Huang, Y.Q., Ju, W., Kalia, L.V., Ahmadian, G., Wang, Y.T., and Salter, M.W. (2003). Glycine binding primes NMDA receptor internalization. Nature *422*, 302–307.

Paton, J.F., Ramirez, J.M., and Richter, D.W. (1994). Mechanisms of respiratory rhythm generation change profoundly during early life in mice and rats. Neurosci. Lett. *170*, 167–170.

Pfeiffer, F., Simler, R., Grenningloh, G., and Betz, H. (1984). Monoclonal antibodies and peptide mapping reveal structural similarities between the subunits of the glycine receptor of rat spinal cord. Proc. Natl. Acad. Sci. USA *81*, 7224–7227.

Prior, P., Schmitt, B., Grenningloh, G., Pribilla, I., Multhaup, G., Beyreuther, K., Maulet, Y., Werner, P., Langosch, D., Kirsch, J., and Betz, H. (1992). Primary structure and alternative splice variants of gephyrin, a putative glycine receptor-tubulin linker protein. Neuron *8*, 1161–1170.

Ramirez, J.M., Quellmalz, U.J., and Richter, D.W. (1996). Postnatal changes in the mammalian respiratory network as revealed by the transverse brainstem slice of mice. J. Physiol. *491*, 799–812.

Richter, D.W., and Spyer, K.M. (2001). Studying rhythmogenesis of breathing: comparison of in vivo and in vitro models. Trends Neurosci. *24*, 464–472.

Ritter, B., and Zhang, W. (2000). Early postnatal maturation of GABAA-mediated inhibition in the brainstem respiratory rhythm-generating network of the mouse. Eur. J. Neurosci. *12*, 2975–2984.

Roux, M.J., and Supplisson, S. (2000). Neuronal and glial glycine transporters have different stoichiometries. Neuron *25*, 373–383.

Sakata, Y., Owada, Y., Sato, K., Kojima, K., Hisanaga, K., Shinka, T., Suzuki, Y., Aoki, Y., Satoh, J., Kondo, H., et al. (2001). Structure and expression of the glycine cleavage system in rat central nervous system. Brain Res. Mol. Brain Res. *94*, 119–130.

Sato, K., Yoshida, S., Fujiwara, K., Tada, K., and Tohyama, M. (1991). Glycine cleavage system in astrocytes. Brain Res. *567*, 64–70.

Schloss, P., Puschel, A.W., and Betz, H. (1994). Neurotransmitter transporters: new members of known families. Curr. Opin. Cell Biol. *6*, 595–599.

Singer, J.H., Talley, E.M., Bayliss, D.A., and Berger, A.J. (1998). Development of glycinergic synaptic transmission to rat brain stem motoneurons. J. Neurophysiol. *80*, 2608–2620.

Smith, J.C., Ellenberger, H.H., Ballanyi, K., Richter, D.W., and Feldman, J.L. (1991). Pre-Botzinger complex: a brainstem region that may generate respiratory rhythm in mammals. Science *254*, 726–729.

Smith, K.E., Borden, L.A., Hartig, P.R., Branchek, T., and Weinshank, R.L. (1992). Cloning and expression of a glycine transporter reveal colocalization with NMDA receptors. Neuron *8*, 927–935.

Spike, R.C., Watt, C., Zafra, F., and Todd, A.J. (1997). An ultrastructural study of the glycine transporter GLYT2 and its association with glycine in the superficial laminae of the rat spinal dorsal horn. Neuroscience *77*, 543–551.

Tada, K., Kure, S., Takayanagi, M., Kume, A., and Narisawa, K. (1992). Non-ketotic hyperglycinemia: a life-threatening disorder in the neonate. Early Hum. Dev. *29*, 75–81.

Verdoorn, T.A., Kleckner, N.W., and Dingledine, R. (1987). Rat brain N-methyl-D-aspartate receptors expressed in *Xenopus* oocytes. Science *238*, 1114–1116.

Xu, F., Gainetdinov, R.R., Wetsel, W.C., Jones, S.R., Bohn, L.M., Miller, G.W., Wang, Y.M., and Caron, M.G. (2000). Mice lacking the norepinephrine transporter are supersensitive to psychostimulants. Nat. Neurosci. *3*, 465–471.

Zafra, F., Aragon, C., Olivares, L., Danbolt, N.C., Gimenez, C., and Storm-Mathisen, J. (1995a). Glycine transporters are differentially expressed among CNS cells. J. Neurosci. *15*, 3952–3969.

Zafra, F., Gomeza, J., Olivares, L., Aragon, C., and Gimenez, C. (1995b). Regional distribution and developmental variation of the glycine transporters GLYT1 and GLYT2 in the rat CNS. Eur. J. Neurosci. *7*, 1342–1352.

Zafra, F., Aragon, C., and Gimenez, C. (1997). Molecular biology of glycinergic neurotransmission. Mol. Neurobiol. *14*, 117–142.

Zhang, W., Barnbrock, A., Gajic, S., Pfeiffer, A., and Ritter, B. (2002). Differential ontogeny of GABA(B)-receptor-mediated pre- and postsynaptic modulation of GABA and glycine transmission in respiratory rhythm-generating network in mouse. J. Physiol. *540*, 435–446.

Zhao, C., Takita, J., Tanaka, Y., Setou, M., Nakagawa, T., Takeda, S., Yang, H.W., Terada, S., Nakata, T., Takei, Y., et al. (2001). Charcot-Marie-Tooth disease type 2A caused by mutation in a microtubule motor KIF1Bbeta. Cell *105*, 587–597.

# Update

Neuron
Volume 41, Issue 4, 19 February 2004, Page 675

DOI: https://doi.org/10.1016/S0896-6273(04)00068-6

Neuron, Vol. 41, 675, February 19, 2004, Copyright ©2004 by Cell Press

# Erratum

## Inactivation of the Glycine Transporter 1 Gene Discloses Vital Role of Glial Glycine Uptake in Glycinergic Inhibition

In Figure 6C of this paper, the ordinate should be labeled *frequency [Hz]* instead of *interval [s]*. Correspondingly, the last sentence on page 789 is incorrect. It should read: "The mean frequency of IPSCs identified in GlyT1$^{-/-}$ neurons (1.7 $\pm$ 1.7 Hz, n = 6) was lower than in wild-type cells (8.6 $\pm$ 6.6 Hz, n = 5; p = 0.03, Figure 6C),..."

**Jesús Gomeza,[1] Swen Hülsmann,[2] Koji Ohno,[1] Volker Eulenburg,[1] Katalin Szöke,[2] Diethelm Richter,[2] and Heinrich Betz[1,*]**
[1]Department of Neurochemistry
Max-Planck-Institute for Brain Research
Deutschordenstrasse 46
60528 Frankfurt
[2]Department of Neuro- and Sensory Physiology
University of Göttingen
Humboldtallee 23
37073 Göttingen
Germany

*Correspondence: neurochemie@mpih-frankfurt.mpg.de